Application of image analysis to evaluate the flocculation process

Mooyoung Han, Tschung-il Kim and Jinho Kim

ABSTRACT

We report a study of how better to evaluate the flocculation process, comparing the image-analyzing method with the turbidity measurement method from a series of jar tests. The size and shape of flocs were measured over a range of velocity gradients (*G*) and flocculation times (*t*). Several advantages of image analysis over the traditional turbidity measurement method were found. Two parameters developed from image analysis, the Feret Diameter (*FD*) and the Shape Factor (*SF*), gave direct information about the characteristics of floc particles whereas turbidity measurement gave only indirect information about the supernatant instead of about the particle itself. The results of image analysis can be obtained in real time whereas turbidity required 30 min of sedimentation time. Image analysis can be used to suggest and evaluate optimum conditions for subsequent processes, such as sedimentation, flotation, membrane and direct filtration, whereas turbidity measurements cannot.

Key words | feret diameter, image analysis, jar test, shape factor, shear condition

Mooyoung Han (corresponding author)
Tschung-il Kim
School of Civil, Urban and Geosystem Engineering,
Seoul National University,
Seoul 151-742,
Korea
E-mail: *myhan@snu.ac.kr*

Jinho Kim
Korea Institute of Industrial Technology,
Seoul 135-51,
Korea

INTRODUCTION

The flocculation process has been used as a pretreatment to reduce the number of small particles, and increase the number of large particles. The properties of the particle after the flocculation process are important because they become the input parameter of the subsequent particle separation process, which include sedimentation, dissolved-air flotation, membrane filtration and direct filtration. Therefore, the evaluation and optimization of the flocculation process is one of the most important processes in water treatment plants (WTPs). Several attempts have been made to find optimum flocculation conditions.

The traditional method in practice is the standard jar test method. The optimum condition is determined by comparing the turbidity of the supernatant after a set of flocculation conditions (*G* and *t*) by 30 min sedimentation. Although *G* does not represent the floc shear strength, and there is discussion of its relative insignificance (Han & Lawler 1992), it is the most widely used parameter in the flocculation process. However, turbidity data are insufficient to provide information on floc properties, because turbidity measurement itself is only an indirect optical measurement. Furthermore, the optimum condition developed from the jar tests is for the combination of both flocculation and sedimentation processes, not for the flocculation process itself. This is important when the subsequent particle separation process is not sedimentation. The time required to do the jar test is also a disadvantage when real time control of the flocculation process is needed.

Particle counting methods were developed to measure the properties of particles. The real time particle size distribution can be measured online. An optimum condition can be defined which fits the target of the flocculation process, i.e. to reduce the number of small particles and increase the number of large particles. However, particle counting yields only the one dimensional size of the particle and so misleading information about the suspension is given

doi: 10.2166/aqua.2006.053

in the case of nonspherical flocs. Also, due to the limitations of the sensor system, large flocs are not counted accurately because of floc breakage (Bower *et al.* 1997; Persson 1998).

With the development of computer equipment and software, it became possible to measure characteristics of the flocs online, in real time and without floc breakage, by taking optical images of a suspension. The shape and particle size distribution can be taken as a picture image and analyzed by appropriate software. Although it has the limitation of measuring only two-dimensional properties, it yields more information than any other method used for the evaluation of the flocculation process.

The purpose of this paper is to define new parameters with which to evaluate floc properties, by using the image analysis method to evaluate the optimum flocculation conditions used in the standard jar test. The results are compared with turbidity measurements made during the same jar test experiments. These results suggest that image analysis gives information that can be used for optimization of the subsequent particle separation process.

EXPERIMENTAL METHOD

Measurement procedure

The image-analyzing method was applied to a standard jar test procedure. Flocculated suspensions of 20 mL were sampled every 300 s using a pipette with a tip of 10 mm diameter, designed to prevent possible floc breakage. Gibbs & Konwar (1982) recommended that pipette tip openings should be larger than 3 mm in order to minimize floc breakage. The sampled suspension was transferred to a plain acrylic cell of dimensions 100 × 100 × 2 (mm) for capturing of the microscopic image. Digital images of 20-fold magnification were captured by a digital camera (Coolpix 4500, Nikon) attached to a microscope (Meiji Techno Co.) and were analyzed to obtain information on floc size, shape, and other properties. Figure 1 is a schematic illustration of the procedure. A similar measurement technique was used by Chakraborti *et al.* (2000, 2003). The available floc size range using this method was 5–1,000 μm. Around 1,000–1,300 flocs were counted in each sampling run. Our computational analysis utilized a commercial program (SigmaScan Pro, SPSS). Because counted floc numbers differ at each sampling, the size distribution is expressed as a percentage of the total population. Turbidities were measured at 300 s intervals using a turbidimeter (2100P, Hach), followed by 30 min sedimentation of flocculated suspensions.

Batch test procedure

The suspension used in the tests was prepared using kaolin powder (50 g) dispersed in deionized water by a high speed laboratory blender for 20 min. This suspension was made up to 1 L with deionized water and allowed to stand for about 1 h. The top 500 mL was carefully decanted, retained and further diluted to 1 L to serve as a stock suspension. It was found that 98% of the particles were below 10 μm and had a mean diameter of 4.54 μm (measured by Coulter Multisizer-II). The diluted suspension had a volume fraction of

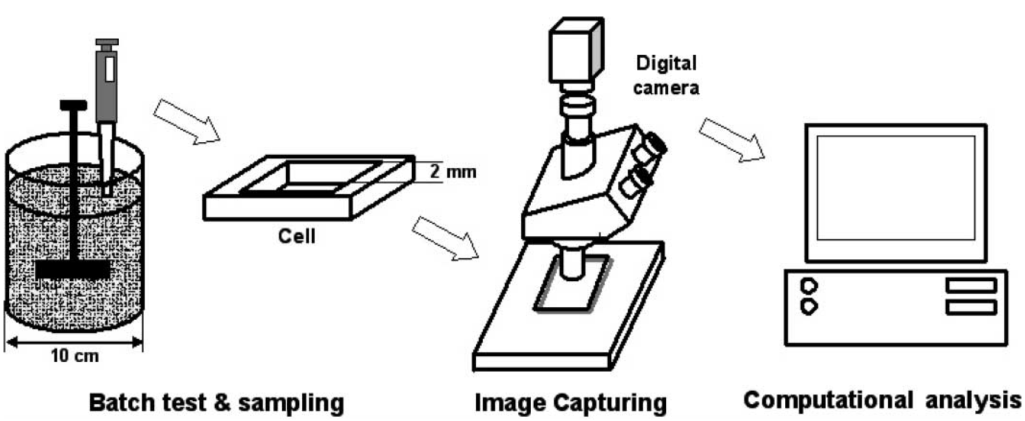

Figure 1 | Schematic illustration of image capturing and analysis procedure.

1.4×10^{-5} ppm and turbidity of 20 NTU. Flocculated tests were done in a 1 L cylindrical vessel of 10 cm diameter. The suspension was mixed using a Rushton type impeller of 76×25 mm. The velocity gradient value is calculated from the relationship of rpm of the impeller (AWWA 1999). The center of the impeller was positioned at 1/3 the height of the vessel.

Acetic acid (CH_3COOH) and sodium bicarbonate ($NaHCO_3$) were used to give an alkalinity of 50 ppm as $CaCO_3$ to the suspension. Sodium bicarbonate ($NaHCO_3$) was used to buffer the suspension and the pH was kept at 7.20 ± 0.05 during all experiments. Alum ($Al_2(SO_4)_3 \cdot 16H_2O$) of 1% (w/v) was used as a coagulant. The coagulant concentration was held constant at 15 mg/L; preliminary jar tests showed that this dosage gave reasonable floc growth. The coagulant was added and the suspension was stirred rapidly ($200\,s^{-1}$) for 30 s to ensure quick and uniform dispersion of alum. After the rapid mixing period, flocculation shear strengths in the range of $45–170\,s^{-1}$ were applied to the suspension for 1,800 s.

RESULTS AND DISCUSSION

Definition of indices

When particles aggregate, the resulting clusters adopt many different and irregular structures. It is not possible to provide a detailed description of their structure. Flocs are now recognized as fractal objects (Meakin 1988) and it is necessary to use simplified forms to define the complicated nature of floc shape. Images of flocs captured by a digital camera show their two-dimensional shape and such morphological characteristics as maximum and minimum sizes, area, and perimeter of the two-dimensional object. In this research, size and shape indices obtained from the relationship between these properties are presented to interpret flocculation behavior (i.e. floc formation and breakage).

Among several ways of defining the floc size, a Feret Diameter is selected as the floc size in this study. It is defined as the average of the longest horizontal and vertical lengths of the particle/floc profile:

$$FD = \frac{(W_{Max} + H_{Max})}{2} \tag{1}$$

where FD is a Feret Diameter, and W_{Max} and H_{Max} are the longest horizontal and vertical lengths respectively (refer to Figure 2 for illustration). For a suspension with many particles, an average value of FD can be obtained from the FD values of each particle in the same picture frame.

There are several ways of defining the external complexity of floc shape, such as the shape factor, form index, and compactness. All these indices use the relationship between the area and the perimeter of the object. Although there may exist some differences in sensitivity between the indices, the trend in variation remains the same. This study employs the shape factor (SF), which is defined as follows:

$$SF = 4\pi \frac{(\text{area})}{(\text{perimeter})^2}. \tag{2}$$

The shape factor becomes close to 1 and 0 when the shape of the object resembles a circle and a line, respectively. The shape factor reflects the two-dimensional compactness of the particle. For a suspension with many particles, an average value of SF can be obtained from the SF values of each particle in the same picture frame.

Result of turbidity measurement

Figure 3(a) shows the residual turbidities after a set of standard jar tests at different velocity gradients (G) and flocculation times (t) followed by 30 min sedimentation. The supernatant turbidities were measured at the same depth in the jars. The range of optimum conditions can be

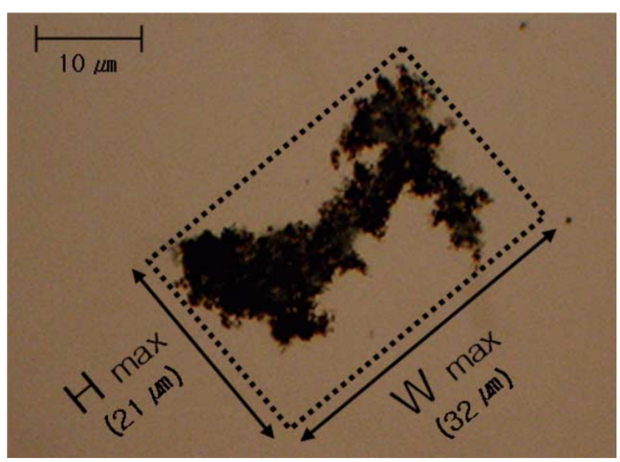

Figure 2 | Definitions of longest width and height for Feret Diameter.

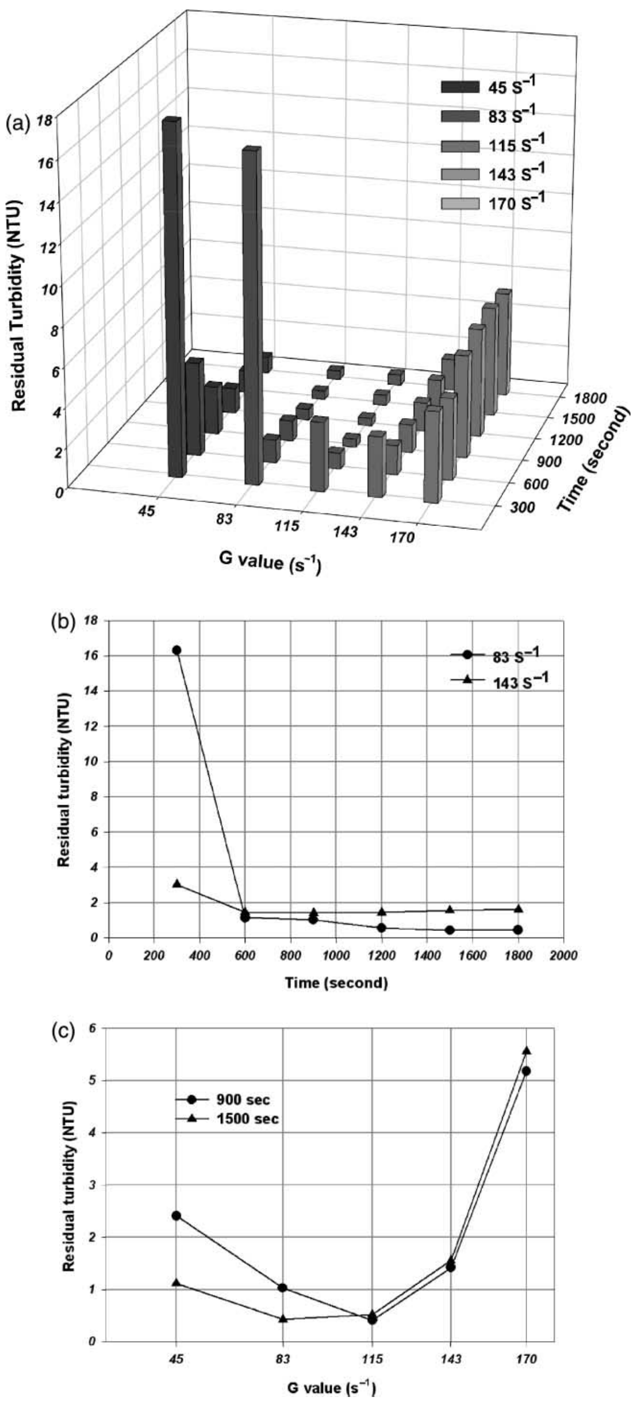

Figure 3 | Turbidity at different flocculation conditions in a standard jar test. (a) Residual turbidity at different flocculation conditions. (b) Relationship between residual turbidity and t value (at $83\,s^{-1}$, $143\,s^{-1}$). (c) Relationship between residual turbidity and G value (at 900 s, 1,500 s).

taken to be those that produce the lowest residual turbidity. These results allow only the turbidity data to be obtained and no data about the properties of the particles are obtained directly.

Two sets of turbidity measurement for velocity gradients of 83 and $143\,s^{-1}$, respectively, are shown to illustrate the effect of flocculation time (Figure 3(b)). Turbidity decreases with time and, after a certain time, remains constant. A possible explanation for this is that there is no effect of particle growth or breakage after this time, but there is no evidence to support this idea.

The effect of velocity gradient is shown for two sets of flocculation times of 900 s and 1,500 s (Figure 3(c)). Initially, the turbidity decreases with increasing velocity gradient, but above a certain velocity gradient the turbidity begins to increase. This might be due to floc breakage at the higher shear strength, leading to more small particles. Small particles do not settle well in the 30 min sedimentation time and contribute to the higher turbidity.

Result of image analysis method

Image analysis was performed during the sets of experiments described above except that the time of sampling from the suspensions was immediately at the end of the flocculation period whereas the turbidity was measured after 30 min sedimentation. Both indices that define the average floc size (*FD*) and shape (*SF*) were measured and the results are shown in Figures 4(a) and 5(a) at different flocculation conditions in a standard jar test. It is axiomatic that the optimum flocculation condition is that which gives the largest floc particles, since these will settle well during sedimentation.

To allow direct comparison with the results of turbidity measurements, the effects on Feret Diameter of two velocity gradients (at $83\,s^{-1}$ and $143\,s^{-1}$) are shown in Figure 4(b). Higher values of *FD* show that the average floc sizes are large. It is observed that the floc size increases with flocculation time and there is a slight decrease in size after reaching a maximum size. The decrease indicates a small amount of floc breakage. It is reported by Brakalov (1987) that floc resistance to breakage by shear decreases with floc size, and this relationship may explain the observed behavior. After the slight decrease in size, a stable

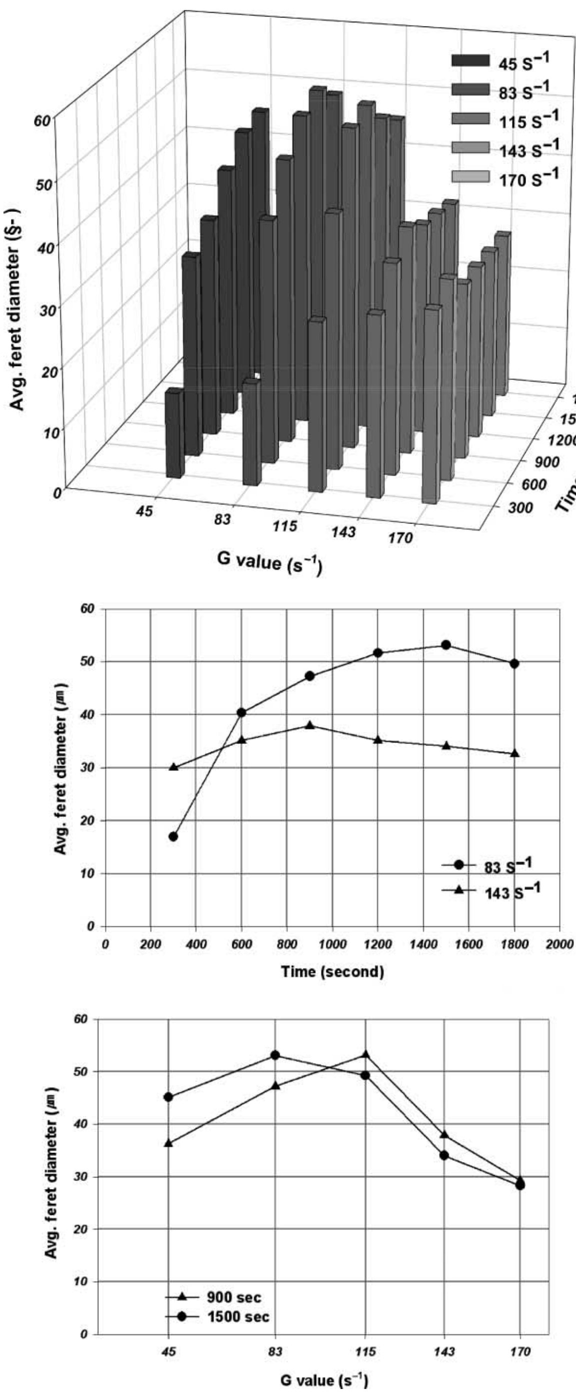

Figure 4 | Feret Diameter at different flocculation conditions by using image analysis. (a) *FD* at different flocculation conditions. (b) Relationship between average *FD* and *t* value (at $G = 83\,s^{-1}$, $143\,s^{-1}$). (c) Relationship between *FD* and *G* value (at 900 s, 1,500 s).

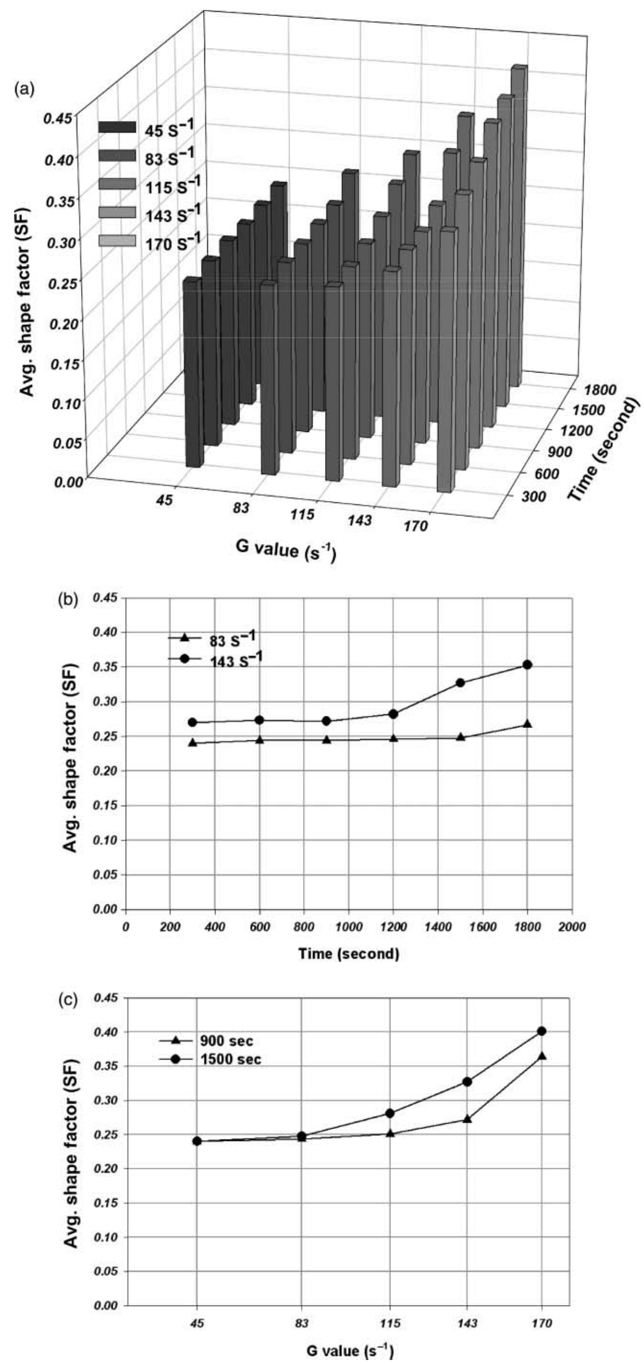

Figure 5 | Shape factor at different flocculation conditions by using image analysis. (a) *SF* at different flocculation conditions. (b) Relationship between average shape factor and *G* value (at $83\,s^{-1}$, $143\,s^{-1}$). (c) Relationship between average shape factor and *G* value (at 900 s, 1,500 s).

particle size is reached (Clark & Flora 1991; Kramer & Clark 1996; Spicer & Pratsinis 1996). This is contrary to the turbidity measurement result which shows no change in the turbidity after a certain time. Again, the effect of velocity gradient for two sets of flocculation times is shown as in Figure 4(c) (cf. Figure 3(c)). There is a decrease of average *FD* at larger velocity gradients, which is a direct indication of floc breakage.

The values of *SF* are shown on the same sets of data (Figure 5(a)). It can be seen that shape factors increase with shear strength and flocculation time. Also it is reported (Wiesner 1992) that fractal dimension was influenced by rapid mixing. For flocs formed within the same period, higher shear strength produces flocs of higher shape factor (i.e. lower compactness). There has been a similar report of such a relationship between the floc density and shear strength as well as the floc density and flocculation time (Kim 2002). The shape factors do not directly match the values of floc density; however, this index provides a good indication of the increasing trend of floc density. Figure 5(b) shows the effect of flocculation time on *SF* at two sets of velocity gradients ($G = 83\,s^{-1}$ and $145\,s^{-1}$). The values of *SF* are constant up to a certain value, after which they gradually increase. The degree of compactness increases with flocculation time. Figure 5(c) shows the effect of velocity gradient. *SF* remains constant up to a certain velocity gradient, after which a gradual increase of SF occurs.

It is interesting to note the combined effect of both *FD* and *SF* under conditions where the turbidity is constant (Figures 3(b), 4(b), and 5(b)). The reason why the turbidity remains constant after a longer period of flocculation time is because the particles become more compact and finally settle better. However, at the higher velocity gradient (Figures 3(c), 4(c), and 5(c)), the turbidity increases at the point where the decrease of *FD* is remarkable. *FD* has more effect than *SF*, which can be possibly explained by Stokes' equation. Because the rate of settling of a single sphere is proportional to the square of the diameter, suspensions which have bigger particles settle better.

Application of image analysis to evaluate the flocculation process

It is important to find the optimum condition for flocculation of a drinking water treatment plant, because this process not only requires significant amounts of energy and chemicals but also affects the optimization of the subsequent process. Therefore, the online particle-based evaluation method is vital for operation of the process. Turbidity measurements by the traditional standard jar test method require time (for sedimentation) and provide limited information about the particle behavior.

Depending on the particle separation process used after flocculation, the desired particle characteristics may be different from each other. For example, the sedimentation process requires large floc particles so that they can be settled within the detention time of the settling tank, whereas the DAF process requires the floc size to be similar to the size of the bubble. Therefore, the optimum condition for sedimentation may be different from that for DAF (Han 2001; Kim 2004). This may be true of other processes. In the membrane process, the required pretreatment may be to produce a floc large enough to be retained behind the pore. For the direct filtration process, the optimum condition is when the floc size is larger than the pore by one order of magnitude, according to the filtration theory suggested by Yao *et al.* (1971).

CONCLUSIONS

In this research, the image analysis method was developed and applied to find the optimum flocculation conditions using standard jars. Two indices (*FD* and *SF*) are defined which represent the size and shape of floc properties, respectively. The results compare well with the traditional turbidity measurement although the image analysis method showed a greater ability to represent the performance of the flocculation process itself. It also uses online measurement, provides more real-time information about the particle characteristics, and can be used to assist other subsequent particle separation processes. When coupled with methods that provide more information on surface characteristics, image analysis will enable optimization of subsequent particle separation processes.

REFERENCES

American Water Works Association 1999 *Water Quality and Treatment*, 5th edn. McGraw-Hill, New York.

Bower, C., Washington, C. & Purewal, T. S. 1997 The use of image analysis to characterize aggregates in a shear field. *Colloids Surf. A: Physicochem. Engng. Aspects* **127**, 105–112.

Brakalov, L. B. 1987 A connection between the orthokinetic coagulation capture efficiency of aggregates and their maximum size. *Chem. Engng. Sci.* **42**, 2373–2383.

Chakraborti, R. K., Atkinson, J. F. & Van Benschonten, J. E. 2000 Characterization of alum floc by image processing. *Environ. Sci. Technol.* **34**(18), 3969–3976.

Chakraborti, R. K., Gardner, K. H., Atkinson, J. F. & Van Benschoten, J. E. 2003 Changes in fractal dimension during aggregation. *Wat. Res.* **37**(4), 885–895.

Clark, M. M. & Flora, J. R. V. 1991 Floc restructuring in varied turbulent mixing. *J. Colloid Interface Sci.* **147**(2), 407–421.

Gibbs, R. J. & Konwar, L. 1982 Effect of pipetting on mineral flocs. *Environ. Sci. Technol.* **16**, 119–121.

Han, M. Y. 2001 Modeling of DAF: the effect of particle and bubble characteristics. *J. Wat. Supply: Res. Techn. – Aqua* **51**(1), 27–34.

Han, M. Y. & Lawler, D. F. 1992 The (relative) insignificance of G in flocculation. *J. AWWA* **84**, 79–91.

Kim, J. 2002 Floc properties in stirred suspensions. PhD dissertation, University of London.

Kim, T. I. 2004 Effects of floc properties on sedimentation and dissolved-air-flotation processes. Master dissertation, Seoul National University.

Kramer, T. A. & Clark, M. M. 1996 The measurement of particles suspended in a stirred vessel using microphotography and digital image analysis. *Part. Syst. Charact.* **13**, 3–9.

Meakin, P. 1988 Fractal aggregates. *Adv. Colloid Interface Sci.* **28**, 249–331.

Persson, A. 1998 Image analysis of shape and size of fine aggregates. *Engng. Geol.* **50**, 177–186.

Spicer, P. T. & Pratsinis, S. E. 1996 Shear-induced flocculation: the evolution of floc structure and the shape of the size distribution at steady state. *Wat. Res.* **30**(5), 1049–1056.

Wiesner, M. R. 1992 Kinetics of aggregate formation in rapid mix. *Wat. Res.* **26**(3), 379–387.

Yao, K.-M., Habibian, M. T. & O'Melia, C. R. 1971 Water and waste water filtration: concepts and applications. *Environ. Sci. Technol.* **5**(11), 1105.

First received 15 March 2006; accepted in revised form 1 July 2006